The Choroid after Half-Dose Photodynamic Therapy in Chronic Central Serous Chorioretinopathy

Evita Evangelia Christou[1,*], Andreas Katsanos[1], Ilias Georgalas[2], Vassilios Kozobolis[3], Christos Kalogeropoulos[1], Maria Stefaniotou[1]

ABSTRACT

Purpose: To characterize choroidal structure and vasculature after half-dose verteporfin photodynamic therapy (hd-vPDT) in eyes with chronic central serous chorioretinopathy using Enhanced Depth Imaging Optical Coherence Tomography (EDI OCT) and Optical Coherence Tomography Angiography (OCT-A).

Methods: This prospective case-control study included 10 eyes. Choroid was examined before and at 1 month following hd-vPDT. We measured choroidal thickness (CT) at subfoveal area and at 750 μm nasal and temporal of fovea and thickness of Haller and choriocapillaris/Sattler layers. Whole (WA), luminal (LA) and interstitial area (IA) at EDI-OCT, and perfusion density at OCT-A were analyzed. The unaffected fellow eyes were used for comparisons.

Results: Mean CT at subfoveal area and at 750 μm nasal and temporal of fovea, values of Haller and choriocapillaris/Sattler layers and those of WA, LA and IA were reduced, while PD increased at 1 month after hd-vPDT (all $p < 0.001$). There was a significant ($p < 0.05$) negative correlation ($\rho = -0.658$) between PD and post-treatment logMARVA. None of analyzed parameters reached values of unaffected fellow eye.

Conclusion: Following hd-vPDT, choroidal thickness with both luminal and interstitial components markedly decreased, while perfusion of choriocapillaris improved.

KEYWORDS

chronic central serous chorioretinopathy; half-dose photodynamic therapy; enhanced depth imaging; optical coherence tomography; optical coherence tomography angiography; PDT

AUTHOR AFFILIATIONS

[1] Department of Ophthalmology, Faculty of Medicine, School of Health Sciences, University of Ioannina, Ioannina, Greece
[2] First Department of Ophthalmology, General Hospital of Athens G. Gennimatas, Medical School, National and Kapodistrian University of Athens, Greece
[3] Department of Ophthalmology, Faculty of Medicine, School of Health Sciences, University of Patras, Patras, Greece
* Corresponding author: University of Ioannina, Faculty of Medicine, Stavrou Niarchou Avenue, 45500, Ioannina, Greece; email: evitachristou@gmail.com

Received: 11 May 2022
Accepted: 14 November 2022
Published online: 2 February 2023

Acta Medica (Hradec Králové) 2022; 65(3): 89–98
https://doi.org/10.14712/18059694.2022.24

INTRODUCTION

Central serous chorioretinopathy (CSC) is a chorioretinal disorder characterized by accumulation of fluid under the neurosensory retina due to dysfunction of the retinal pigment epithelium (RPE) (1–4). A multimodal imaging approach has proposed that CSC in fact belongs to the pachychoroid spectrum of disorders, and the choroidal vascular hyperpermeability is the main pathophysiological feature (5–8). Novel techniques have provided new insights in the visualization of the choroidal structure and circulation. Optical Coherence Tomography using the Enhanced Depth Imaging (EDI-OCT) mode allows us to highlight increased choroidal thickness and dilated large vessels in CSC (9–13). Optical Coherence Tomography Angiography (OCT-A) provides detailed information regarding the retinal and choroidal vascular layers and is useful for the analysis of perfusion changes (6, 7, 14, 15). The use of depth-resolved imaging methods provides evidence of the pathogenic mechanism of CSC during the course of the disease and after treatment (8–15). Verteporfin photodynamic therapy (vPDT) for the treatment of chronic cases has been proven to be an efficacious option. It has been successfully used to reduce choroidal vascular congestion and hyperpermeability (16–19). Recent studies have reported safety-enhanced protocols, in an attempt to minimize potential complications of standard vPDT such as choroidal ischemia, retinal pigment epithelium atrophy, choroidal neovascularization (CNV). Indeed, half-dose or low-fluence modified protocols have been found to be effective and safe in anatomical and functional outcomes regarding resolution of subretinal fluid (SRF), visual acuity (VA) and choroidal perfusion (20, 21).

The aim of this prospective study was to perform a quantitative analysis of choroidal structure including luminal and interstitial components and to analyze vascular changes of the choriocapillaris (CC) before and after applying half-dose vPDT (hd-vPDT) in patients with chronic CSC.

MATERIAL AND METHODS

STUDY DESIGN

The study was conducted at the Department of Ophthalmology of the University of Ioannina, Greece, between September 2020 and March 2021 after receiving approval from the institutional ethics committee (gm 3/24N2020). The investigation adhered to the tenets of the Declaration of Helsinki. Informed consent was obtained from each patient before any study-related activity.

This was a prospective comparative study. Patients who underwent hd-vPDT for chronic CSC were recruited and their data were analyzed. Inclusion criteria were: a) diagnosis of chronic CSC, b) a single successful treatment with hd-vPDT, c) complete EDI-OCT and OCT-A data before vPDT (at baseline within 1 week from treatment) and at 1 month post-treatment. Eyes with a history of previous ocular surgery other than uncomplicated phacoemulsification, trauma, high refractive errors, co-existent macular and vitreoretinal pathology were excluded to avoid potential confounding effects. In addition, we excluded eyes that had previously received any form of therapy (vPDT, laser photocoagulation, intravitreal injections of anti-vascular endothelial growth factor/VEGF) or those with evidence of CNV secondary to CSC. Patients with low quality images were also excluded. The patients' unaffected fellow eyes were used for comparisons.

All participants underwent a comprehensive eye examination that included measurement of best corrected visual acuity, determination of intraocular pressure, slit-lamp biomicroscopy and fundus examination after pupil dilation. The indication for applying vPDT was chronic CSC with persistent SRF of at least 3 months duration and foveal involvement that was confirmed by active angiographic leakage in fluorescein angiography and choroidal vascular hyperpermeability in indocyanine green angiography. EDI-OCT and OCT-A imaging were performed at baseline and at 1 month after treatment.

EDI-OCT AND OCT-A IMAGING PROTOCOLS

SD-OCT (Cirrus HD-OCT, Zeiss, Jena, Germany) using the eye-tracking system was performed to investigate the choroidal area. The scans were acquired with the EDI mode at baseline and at 1 month after applying vPDT. Choroidal thickness (CT) was measured at the subfoveal area and at 750 μm to the nasal and temporal sides of the fovea. The Haller's layer and the Sattler's/CC layer were assessed independently. Choroidal layer analysis of the OCT images were manually performed based on previously described methods (22). Choroidal thickness measurements were performed using as landmarks the distance from the outer portion of the hyper-reflective line which corresponds to the Bruch's membrane, and the inner hyper-reflective line of the choroid-sclera interface. The cut-off size of the large choroidal vessels in the horizontal images through the fovea was selected at 100 μm. Choroidal vessels located closest to the center of the fovea having a diameter larger than 100 μm were used for the measurements. The latter defined the horizontal line from the innermost point of the large choroidal vessels that intersected the subfoveal CT measurement line perpendicularly. The subfoveal choroidal large vessel layer thickness was defined as the distance from the point of intersection on the subfoveal CT line to the inner surface of the sclera. The thickness of the Sattler's/CC layer was derived by subtracting the thickness of the Haller's layer from the subfoveal CT. All EDI-OCT images were imported in Image J. A 1500 μm wide area under the fovea (750 μm nasally and temporally to the center) extending vertically from the RPE to the chorioscleral border was selected for analysis. The scans were thresholded by an Otsu method and analyzed by binarization technique (7, 14). The white zones corresponded to the interstitial spaces and the black zones to the luminal area. The whole area (WA), luminal area (LA) and interstitial area (IA) of the choroid were calculated. A ratio between luminal part and total choroid corresponding to the choroidal vascularity index (CVI) in former studies was measured (23). The measurements for the images were obtained by the same examiner. All images were obtained at approximately 10 am to avoid the influence of diurnal choroidal changes.

OCT-A generates high-resolution three-dimensional maps of the retinal and choroidal microvasculature. Imaging was performed with the AngioPlex® OCT Angiography (ZEISS, Jena, Germany), and OCT angiograms were acquired in a 6 × 6 mm scan pattern automatically centered at the fovea. En face images of the CC plexus were generated and automated layer segmentation was performed by the software using a slab between 29 and 49 µm below the RPE reference. The automated slab segmentation was checked and manually corrected in case of inaccuracy. Each OCT angiogram at the CC layer was imported in Image J for analysis. Binarization of the images was made by the Otsu method, which is an automatic threshold selection from gray-level histograms. Contrary to the EDI-OCT scans, the white zones corresponded to the lumen of vessels of the CC network and the black zones to the interstitial area. We assumed that the percentage of white zones was an indirect measure of the choroidal vascular flow area of the CC, therefore the percentage area occupied by the microvasculature in the CC layer defined the perfusion density. Indeed, a ratio between luminal part and total area in the CC layer was equivalent to the vascular density in previous studies (14). All scans were reviewed to ensure their quality was sufficient.

HALF-DOSE VPDT PROTOCOL

The participants were subjected to the modified protocol of hd-vPDT. Verteporfin was administrated intravenously at a dose of 3 mg/m² over 10 minutes. Fifteen minutes after the initial verteporfin infusion, the treatment area was exposed to a delivery of diode laser of 689 nm with a fluence of 600 mw/cm² for 83 seconds and total laser energy of 50 J/cm² using a contact lens (Volk Area Centralis). The spot size had a diameter of 1000 µm larger than the greatest linear dimension of the choroidal exudation in indocyanine green angiography (ICGA). Patients were advised to avoid exposure to sunlight for 48 h post-treatment due to a potential risk of skin photosensitivity.

STATISTICAL METHODOLOGY

We performed the statistical analysis using SPSS version 25.0 (SPSS Inc., Chicago, IL, USA). Continuous variables were expressed as mean ± standard deviation (SD). We used the paired t-test for normally distributed data, or the Mann-Whitney U test for non-normally distributed data. To examine the correlation of two continuous variables, we used the Pearson coefficient for normally distributed data, or the Spearman coefficient for non-normally distributed data. Normality was tested using the Shapiro-Wilks test. For all tests, statistical differences were determined to be significant at $p < 0.05$.

RESULTS

We examined 17 patients (19 eyes) with chronic CSC. After exclusion criteria a total of ten eyes of 10 patients (8 men, 2 women) who underwent hd-PDT were included in the study. We excluded 2 eyes with residual SRF at first month after treatment, 2 eyes with evidence of CNV, 3 eyes which had received previous treatment (1 with vPDT, 2 with anti-VEGF injections) and a patient with systemic contraindications to verteporfin. The mean age of the patients was 44.70 ± 5.72 years (range: 37–56). The mean period between diagnosis of CSC and applying treatment was 22.40 ± 3.20 months (range: 18–29). All eyes included in the analysis had complete resolution of SRF at 1 month post-treatment. We analyzed the EDI-OCT and OCT-A characteristics at baseline and at 1 month after hd-vPDT. The patients' descriptive characteristics expressed in mean ± SD are shown in table 1.

EDI-OCT CHOROIDAL VALUES

The measurements of the CT at the subfoveal area and at 750 µm nasal and temporal of the center after treatment were significantly lower compared to those before (all $p < 0.001$). Moreover, treated eyes at baseline had signifi-

Tab. 1 Descriptive characteristics of affected and unaffected fellow eyes. Data presented as mean ± standard deviation.

	affected before PDT	affected after PDT	unaffected fellow
SFCT (µm)	411.50 ± 34.74	307.30 ± 17.96	297.30 ± 19.60
750N CT (µm)	375.60 ± 33.53	290.40 ± 18.33	280.60 ± 16.81
750TCT (µm)	391.00 ± 33.21	299.10 ± 18.68	288.50 ± 17.60
Haller (µm)	329.20 ± 38.80	215.30 ± 15.84	202.20 ± 17.65
CC+Sattler (µm)	82.30 ± 16.89	92.00 ± 18.01	95.70 ± 18.06
EDI-OCT whole area (mm²)	944197.00 ± 37291.06	684814.50 ± 25568.83	666526.50 ± 17657.02
EDI-OCT luminal area(mm²)	649590.10 ± 36586.50	288724.90 ± 25281.89	464548.50 ± 20683.03
EDI-OCT interstitial area(mm²)	294606.90 ± 19163.4	196089.60 ± 31901.30	201978.00 ± 22301.40
CVI (%)	0.69 ± 0.02	0.71 ± 0.04	0.70 ± 0.03
perfusion (%)	48.29 ± 1.89	50.56 ± 1.75	51.27 ± 1.57
visual acuity (logMAR)	0.56 ± 0.23	0.49 ± 0.25	0.14 ± 0.05

Abbreviations: PDT – photodynamic therapy; SFCT – subfoveal choroidal thickness; CT – choroidal thickness; EDI-OCT – enhanced depth imaging optical coherence tomography; CVI – choroidal vascularity index

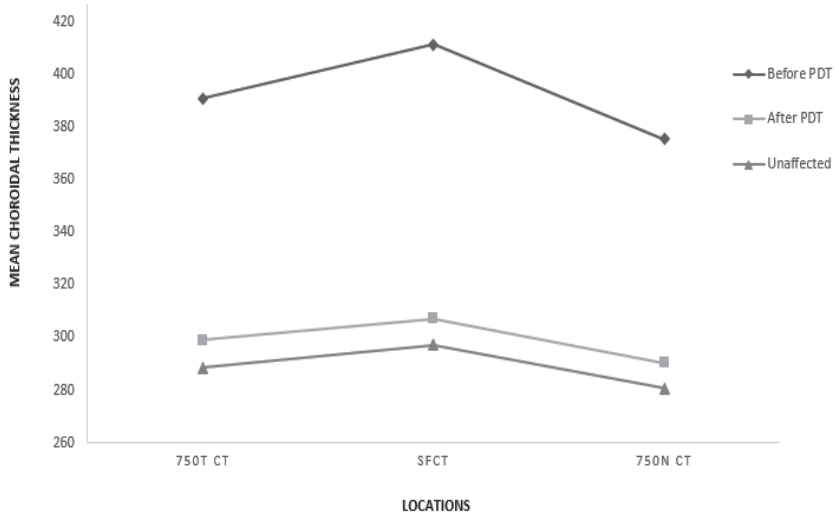

Fig. 1 Choroidal thickness values in affected eyes before and after photodynamic therapy (PDT) and in fellow eyes.

Legend 1: Mean subfoveal choroidal thickness (SFCT) and mean choroidal thickness at 750µm temporal (750T CT) and nasal (750N CT) of the fovea. Mean values before PDT: SFCT = 411.50, 750N CT = 375.60, 750T CT = 391.00; after PDT: SFCT = 307.30, 750N CT = 290.40, 750T CT = 299.10; unaffected fellow: SFCT = 297.30, 750N CT = 280.60, 750T CT = 288.50; $p \leq 0.001$ in all cases.

cantly higher measurements of the CT at each region compared to the fellow eyes (all $p < 0.001$), while after treatment the measurements remained higher than those of the contralateral eye (all $p < 0.001$) (Figure 1). After vPDT, the thickness of Haller's and CC/Sattler's layers was significantly lower compared to those before treatment (all $p < 0.001$). Moreover, treated eyes at baseline had significantly higher measurements of the choroidal layers compared to the fellow eyes (all $p < 0.001$), while after treatment the thickness measurements of Haller's and CC/Sattler's remained higher than those of the contralateral eye ($p = 0.005$ and $p < 0.001$, respectively) (Figure 2). The binarized EDI-OCT images indicated markedly lower values of the total area of the choroid, as well as the luminal and interstitial components after treatment compared to baseline (all $p < 0.001$). In addition, treated eyes at baseline had markedly higher values of WA, LA, and IA compared to the fellow eyes (all $p < 0.001$). Following vPDT, the values remained higher than those of the contralateral eyes (all $p < 0.001$) (Figure 3). Regarding the CVI, the mean values before vPDT did not differ significantly compared to those following treatment ($p = 0.148$). CVI of treated eyes before vPDT did not differ statistically from that of the fellow eyes ($p = 0.491$). The mean values of CVI post-treatment were significantly higher than those of the fellow eyes ($p = 0.043$).

OCT-A CC VALUES

The values of the perfusion at the CC layer following vPDT were significantly higher compared to those before treatment ($p < 0.001$). Moreover, treated eyes before vPDT had statistically significant lower values of the CC perfusion compared to the fellow eyes ($p < 0.001$), while the post-treatment values did not reach the level of the contralateral eye ($p < 0.001$) (Figure 4).

VISUAL OUTCOMES

Visual outcomes after vPDT significantly improved compared to pre-treatment measurements ($p = 0.039$). However, the post-treatment VA did not reach the level of the contralateral eye ($p = 0.005$). Correlation analyses revealed that both pre-treatment and post-treatment VA correlated in a significantly negative way to the perfusion values of the CC ($p = 0.028$ and $p = 0.038$, respectively) (Figure 5).

DISCUSSION

Herein, we report microstructural and microcirculation changes in eyes with chronic CSC after applying hd-vPDT. Using a morphometric analysis of binarized EDI-OCT B-scans and en face OCT angiograms, we evaluated vascular and stromal alterations of the total choroidal area and flow changes of the CC network at 1 month post-treatment. It has been largely demonstrated that modified safety-enhanced treatment protocols are efficient in the amelioration of functional outcomes and the restoration of retinal architecture. Indeed, vPDT with a reduced dose of verteporfin or a shortened time of laser emission still achieve satisfactory treatment efficacy with a diminished hypoxic effect on choroidal circulation (20, 21). In the study by Chan et al. (8), the potential of a temporary short-term CC hypoperfusion followed by vascular remodeling and improvement of blood circulation over time has been speculated. Histopathologically, occlusion of the CC has been observed in human eyes 1 week post-vPDT followed by vascular recanalization (24), while reperfusion in the normal choroid may occur within 7 weeks (25). The introduction of novel depth-resolved imaging modalities, including the techniques of EDI-OCT and OCT-A, has provided new insights in the visualization of the chorioretinal morphology and microcirculation. A number of series have revealed variability in qualitative and quantitative analyses of flow pattern, luminal and interstitial components and perfusion evaluated during the post-treatment follow-up period (9–15). Changes in the choroid, and specifically the CC plexus, may indicate the treatment impact on choroidal tissue remodeling and imply the potential of anatomical and functional recovery (6–15).

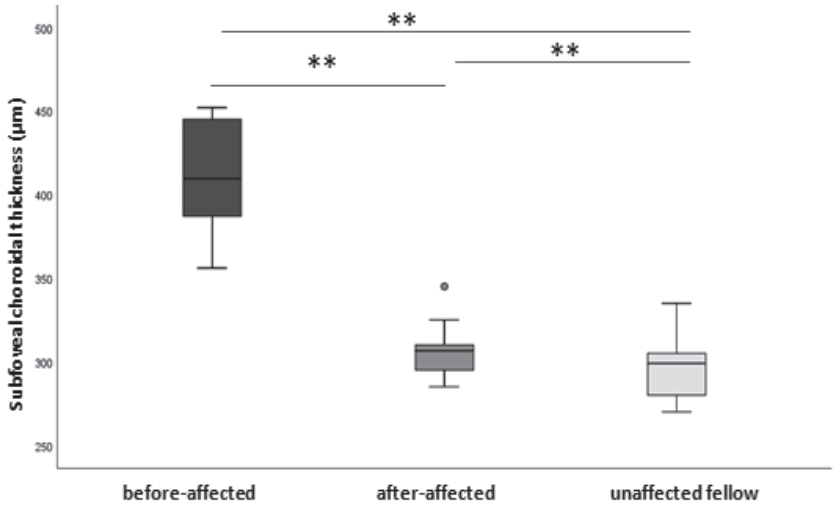

Fig. 2a Subfoveal choroidal thickness values in affected and fellow eyes.

Legend 2a: Means plot Subfoveal choroidal thickness (µm) from affected eyes (before-affected, after-affected) and fellow eyes (unaffected fellow). Mean values SFCT: before PDT = 411.50, after PDT = 307.30, unaffected fellow = 297.30, **p<0.001.

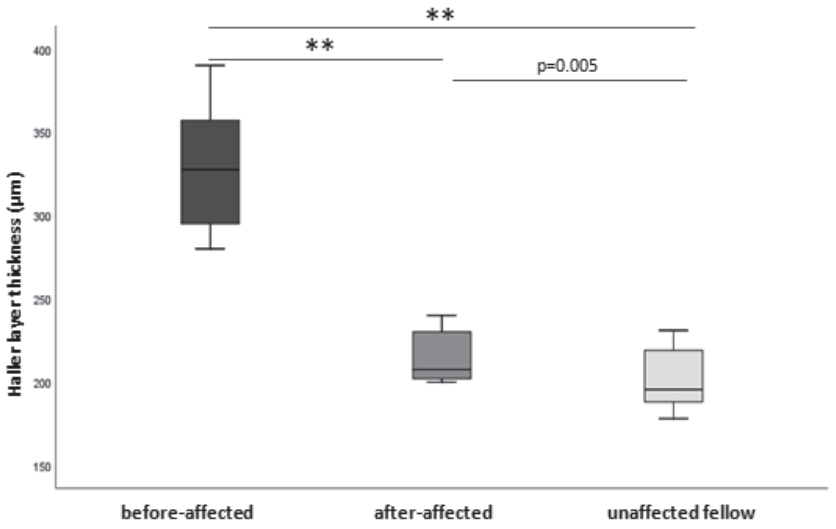

Fig. 2b Haller layer thickness values in affected and fellow eyes.

Legend 2b: Means plot Haller layer thickness (µm) from affected eyes (before-affected, after-affected) and fellow eyes (unaffected fellow). Mean values Haller: before PDT = 329.20, after PDT = 215.30, unaffected fellow = 202.20, **p < 0.001.

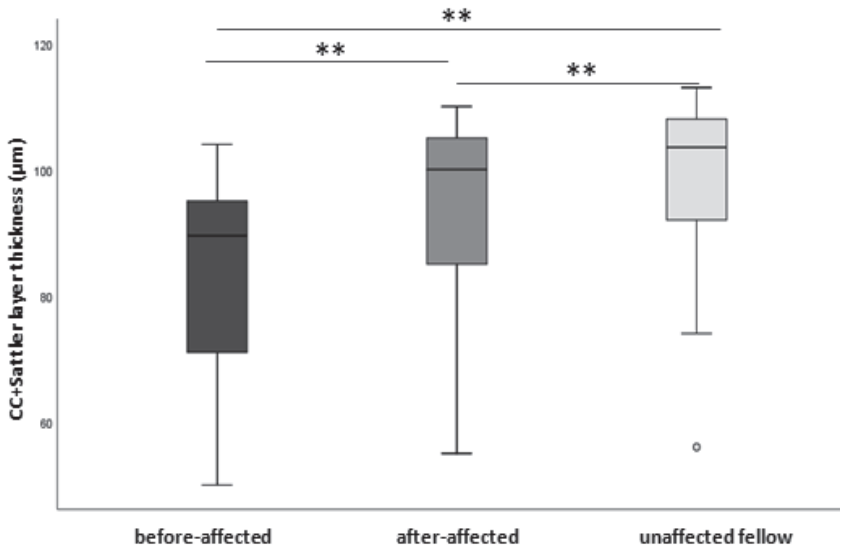

Fig. 2c Choriocapillaris (CC) + Sattler layer thickness values in affected and fellow eyes.

Legend 2c: Means plot Choriocapillaris (CC) + Sattler layer thickness (µm) from affected eyes (before-affected, after-affected) and fellow eyes (unaffected fellow). Mean values CC+Sattler: before PDT = 82.30, after PDT = 92.00, unaffected fellow = 95.70, **p < 0.001

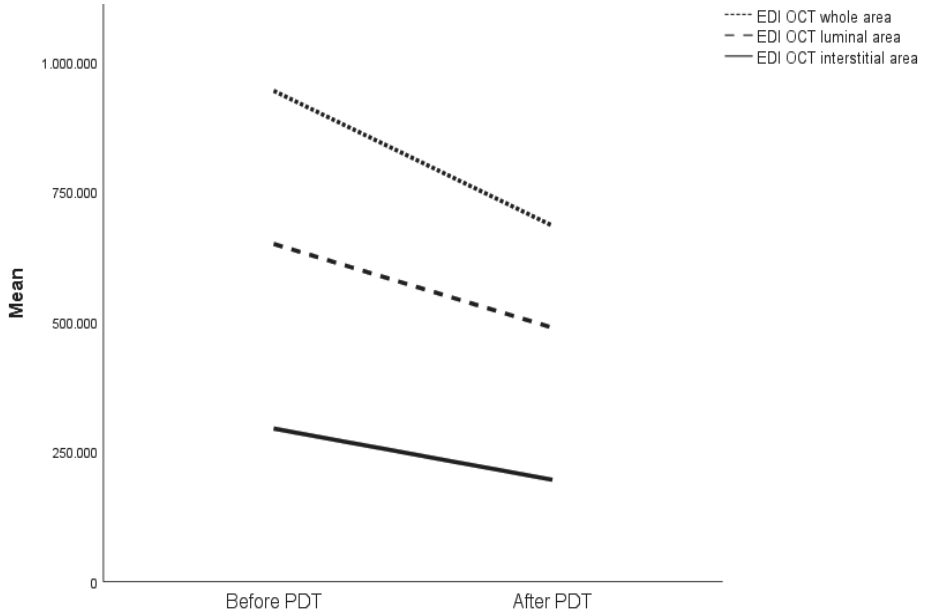

Fig. 3a Choroidal area at enhanced depth imaging Optical Coherence Tomography (EDI-OCT) in affected eyes before and after photodynamic therapy (PDT).

Legend 3a: Change of mean choroidal area (whole, luminal and interstitial) in affected eyes before and after PDT. Mean values whole: before PDT = 994197.00, after PDT = 684814.50, unaffected fellow = 666526.50; luminal: before PDT = 649590.10, after PDT = 288724.90, unaffected fellow = 464548.50; interstitial: before PDT = 294606.90, after PDT = 196089.60, unaffected fellow = 201978.00; $p \leq 0.001$ in all cases.

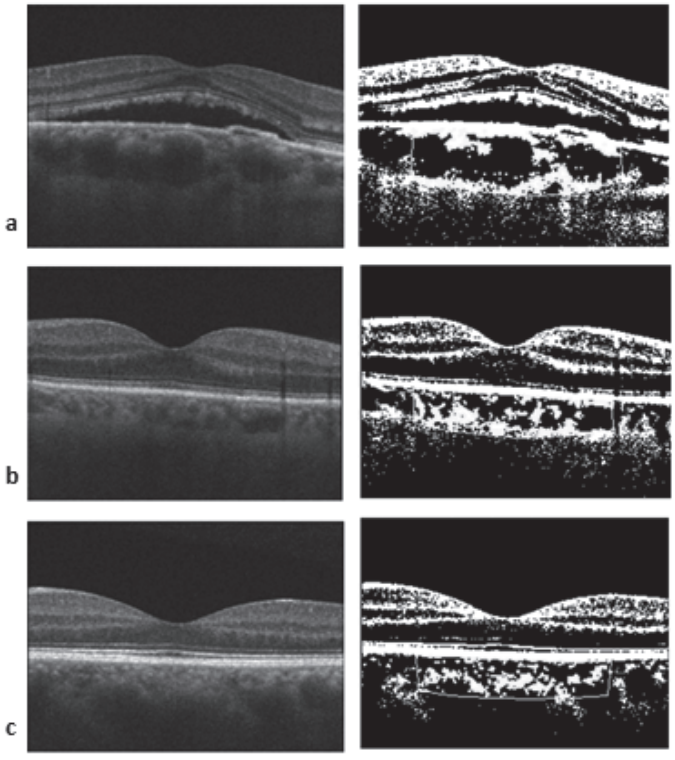

Fig. 3b EDI-OCT images of affected and fellow eye.

Legend 3b: a) EDI-OCT image (left) and binarized image (right) of affected eye before PDT, b) EDI-OCT image (left) and binarized image (right) of affected eye after PDT, c) EDI-OCT image (left) and binarized image (right) of unaffected fellow eye.

In the present study, we investigated the functional and anatomic outcomes occurring after hd-vPDT, focusing especially on the choroidal vasculature. Our results indicated changes regarding the choroidal structure components after treatment. The values of CT at each measured area (subfoveal, 750μm nasally as well as temporally off the center) using EDI-OCT were significantly decreased at 1 month after vPDT compared to those before treatment, as previously described. However, the CT of the affected eye even after vPDT was higher than that of the contralateral eye. Indeed, the comparison of the CT measurements on both eyes of patients with unilateral disease at a 12-month follow-up period has indicated that the CT in vPDT-treated eyes remained thicker than that of the contralateral eye (26, 27), with the amount of choroidal thinning being significantly greater after full-fluence vPDT as compared to modified protocols (28). Authors of previous studies have commented that choroidal thinning following vPDT should be considered in the context of normalization of the pathologically increased choroid, and that the treatment effect does not go beyond the remodeling process, and therefore does not lead to choroidal atrophy (29). Of note, concerning measurements of Haller and CC/Sattler layer thickness, our results support a significant decline in both layers post-treatment. Regarding the thickness of individual choroidal layers, the existing evidence does not unequivocally specify which layers are most affected: some papers have only documented the decrease of total choroidal thickness (20, 27, 28), while others have found a decrease of individual layers (9, 13, 21).

We further examined the whole choroidal area and its components using the binarization process. The reduction of WA we found in our study may reflect the decrease in CT. Previous publications have reported shrinkage of the total choroidal volume with controversial outcomes concerning the luminal and stromal components (9–13). A reduction of the luminal part may confirm the hypothesis

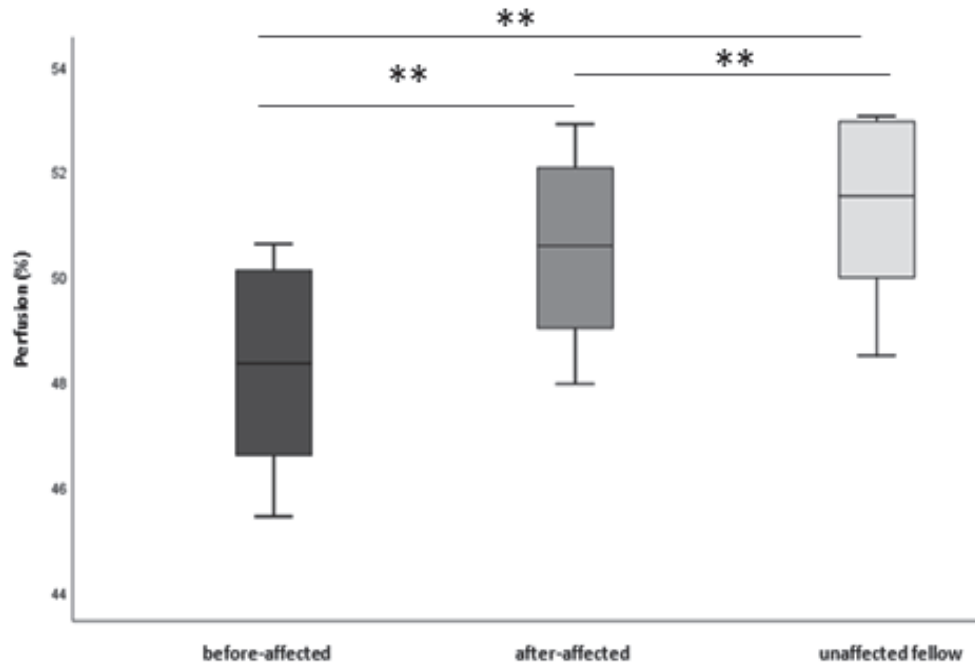

Fig. 4a Perfusion values in affected and fellow eyes.

Legend 4a: Means plot perfusion (%) from affected eyes (before-affected, after-affected) and fellow eyes (unaffected fellow). Mean values perfusion: before PDT = 48.29, after PDT = 50.56, unaffected fellow = 51.27, **p < 0.001.

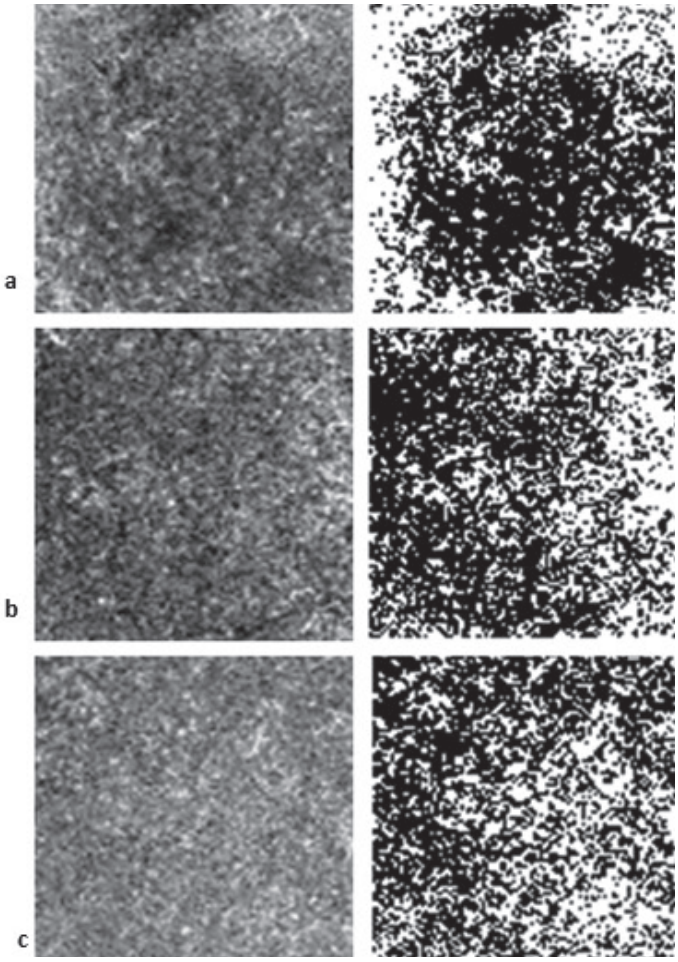

Fig. 4b OCT-A images of affected and fellow eye.

Legend 4b: a) OCT-A image (left) and binarized image (right) of affected eye before PDT, b) OCT-A image (left) and binarized image (right) of affected eye after PDT, c) OCT-A image (left) and binarized image (right) of unaffected fellow eye.

that vPDT has a direct effect on large choroidal vessels as the main treatment target, which results in decongestion of CC vessels and eventual vascular flow re-establishment with a secondary modification on CC compression and vascular flow amelioration. Apart from the significant reduction of the vascular luminal area, our study demonstrated a simultaneous reduction of the interstitial part. The decrease of both choroidal vascular and extravascular components implies that the effect of vPDT on choroidal tissue may involve vascular decongestion as well as interstitial fluid absorption. The CVI is a novel parameter to quantitatively describe the choroidal vasculature demonstrating the ratio of LA over WA (23). In our study, both LA and WA were reduced after vPDT treatment, thus offering a potential explanation why CVI did not markedly differ compared to that at baseline.

Our analysis of OCT angiograms by the binarization method has mainly focused on the perfusion changes of the CC layer following vPDT. The flow pattern and vascular perfusion changes have been initially analyzed in a qualitative way followed by further precise quantification (30–34). Previous studies have mentioned an aberrant flow pattern at the CC layer in eyes before receiving vPDT with a tendency to recovery and a relatively uniform flow after the absorption of SRF at 1 month post-treatment, just as in our study (30–32, 34). Contrary to these results, Teussink et al (6) mentioned an aberrant CC vasculature that persisted even after the absorption of SRF, and appeared to be independent of the therapy used. This discrepancy among the results of these studies may be due to the difference in the period between the provided treatment and the OCT-A examination. Teussink and co-authors (6) may have missed any primary therapeutic effect seen on OCT-A. On the other hand, studies lacking long-term follow-up would have not confirmed a potential recurrent

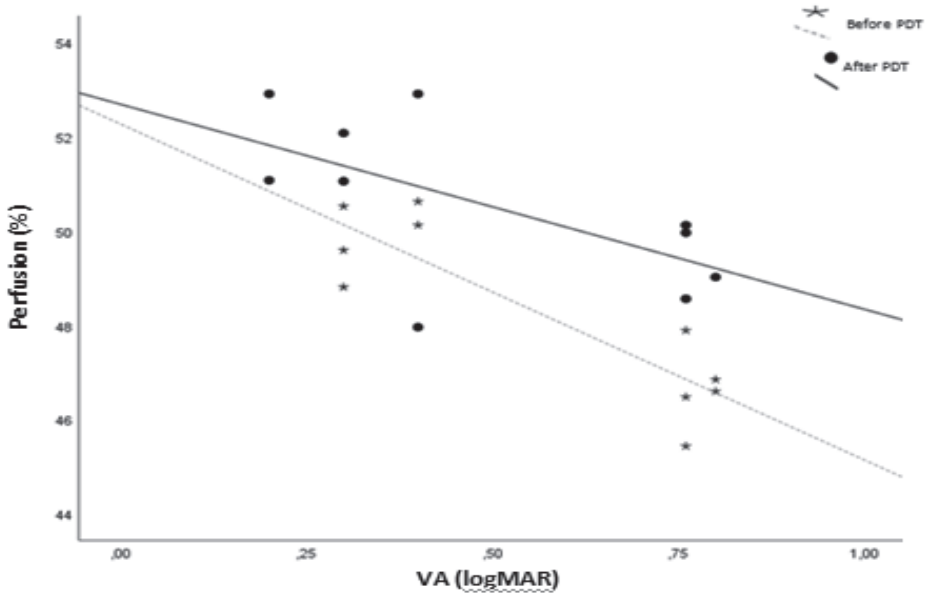

Fig. 5 Correlation analysis between perfusion and visual acuity (VA) before and after photodynamic therapy (PDT) in affected eyes.
Legend 5: Significantly negative correlation between perfusion and VA before and after PDT in affected eyes (before PDT: $\rho = -0.688$, $p = 0.028$; after PDT: $\rho = -0.658$, $p = 0.038$).

the compression on the CC layer. In fact, the overexpression of VEGF at the treatment site due to potential tissue hypoxia may consequently contribute to an increase in vascular density in deep capillary plexus and CC related to the process of recovery. The restoration of the latter vascular networks that constitute the main nutrient and oxygen supply of photoreceptors, leads to resultant photoreceptor recovery and visual acuity improvement (36). Analyzing the OCT angiograms by the binarization method in our study, the percentage area occupied by the microvasculature in specific regions defined the perfusion density. Consequently, our results support the hypothesis that the recovery of CC perfusion leads to photoreceptor restoration, which is in turn associated with functional improvement.

To date, there is limited evidence for the association between CC perfusion changes and VA after vPDT in patients with CSC. We consider this information highly relevant for clinical practice, as perfusion changes could possibly serve as a predicting factor for visual outcomes. Our study contributes to a little-studied issue which undoubtedly warrants further investigation. Certain limitations of the current study need to be considered. Firstly, our patients were examined at only one time-point after vPDT. Obviously, any short-term changes may have been missed. In addition, our results may not accurately portray the choroidal vascular and structural characteristics over the long-term. We intend to follow our patients in order to detect further morphometrical and functional changes over time. Secondly, the sample size was relatively small. Nonetheless, even this small sample enabled the detection of significant differences in several of the investigated parameters. Conceivably, more subtle effects could have been detected using a larger sample. Thirdly, the patients' fellow unaffected eyes were used as controls. One could suggest that contralateral eyes of patients with CSC should not be considered normal, as differences have been found when compared to healthy controls (37). However, using different participants as controls could also be problematic, as the eyes of different people me have important physiological differences. In addition, we should not ignore the intrinsic limitations of the imaging technology used. It can be argued for instance, that a swept-source system would be more appropriate than a spectral-domain device for the visualization of the CC and the choroidal area. On the other hand, it was recently shown that both swept-source and spectral-domain systems are comparable for choroidal measurements (38). Lastly, it should be noted that our results were produced using a well-known image-processing software and a procedure (binarization) that has been used for similar studies (7, 13, 14, 31, 34, 39). Theoretically, employing different imaging platforms and processes could have produced different results.

CONCLUSION

EDI-OCT and OCT-A improves our knowledge on the pathophysiology of choroidal circulation and morphologic changes induced by hd-vPDT in chronic CSC. Quantification of choroidal components may highlight the anatomic response of the tissue to treatment with hd-vPTD. The increase of perfusion density in OCT angiographic findings following treatment may signify functional improvement.

DECLARATIONS

All authors meet the International Committee of Medical Journal Editors (ICMJE) criteria for authorship for this article, take responsibility for the integrity of the work as a whole, and have given their approval for this version to be published.

COMPETING INTERESTS

Andreas Katsanos has to report lecture fees and congress expenses by Santen, Vianex, Zwitter and research grant by Laboratoires Thea. The other authors have no disclosures to report.

FUNDING

No funding or sponsorship was received for this study.

DATA AVAILABILITY

All data will be available upon reasonable request.

REFERENCES

1. Prünte C, Flammer J. Choroidal capillary and venous congestion in central serous chorioretinopathy. Am J Ophthalmol 1996 Jan; 121(1): 26–34.
2. Katsanos A, Gorgoli K, Konidaris V, Empeslidis T. An overview of risk factors, diagnosis and treatment of central serous chorioretinopathy. In: Patrick Evans (Ed). Central serous chorioretinopathy (CSCR): risk factors, diagnosis and management. Chapter 1, p: 1–32. Nova Science Publishers Inc, NY, USA, 2017.
3. Piccolino FC, de la Longrais RR, Ravera G, et al. The foveal photoreceptor layer and visual acuity loss in central serous chorioretinopathy. Am J Ophthalmol 2005 Jan; 139(1): 87–99.
4. Spaide RF, Campeas L, Haas A, et al. Central serous chorioretinopathy in younger and older adults. Ophthalmology 1996 Dec; 103(12): 2070–9; discussion 2079–80.
5. Cheung CMG, Lee WK, Koizumi H, Dansingani K, Lai TYY, Freund KB. Pachychoroid disease. Eye (Lond) 2019 Jan; 33(1): 14–33.
6. Teussink MM, Breukink MB, van Grinsven MJ, et al. OCT Angiography Compared to Fluorescein and Indocyanine Green Angiography in Chronic Central Serous Chorioretinopathy. Invest Ophthalmol Vis Sci 2015 Aug; 56(9): 5229–37.
7. Sonoda S, Sakamoto T, Yamashita T, et al. Choroidal structure in normal eyes and after photodynamic therapy determined by binarization of optical coherence tomographic images. Invest Ophthalmol Vis Sci 2014 Jun 3; 55(6): 38939. Erratum in: Invest Ophthalmol Vis Sci 2014 Aug; 55(8): 4811–2.
8. Chan WM, Lam DS, Lai TY, Tam BS, Liu DT, Chan CK. Choroidal vascular remodelling in central serous chorioretinopathy after indocyanine green guided photodynamic therapy with verteporfin: a novel treatment at the primary disease level. Br J Ophthalmol 2003 Dec; 87(12): 1453–8.
9. Flores-Moreno I, Arcos-Villegas G, Sastre M, Ruiz-Medrano J, Arias-Barquet L, Duker JS, Ruiz-Moreno JM. Changes in choriocapillaris, sattler, and haller layer thicknesses in central serous chorioretinopathy after half-fluence photodynamic therapy. Retina 2020 Dec; 40(12): 2373–8.
10. Hua R, Liu L, Li C, Chen L. Evaluation of the effects of photodynamic therapy on chronic central serous chorioretinopathy based on the mean choroidal thickness and the lumen area of abnormal choroidal vessels. Photodiagnosis Photodyn Ther 2014 Dec; 11(4): 519–25.
11. Razavi S, Souied EH, Cavallero E, Weber M, Querques G. Assessment of choroidal topographic changes by swept source optical coherence tomography after photodynamic therapy for central serous chorioretinopathy. Am J Ophthalmol 2014 Apr; 157(4): 852-60.
12. Chung YR, Kim JW, Kim SW, Lee K. Choroidal thickness in patients with central serous chorioretinopathy: Assessment of Haller and Sattler Layers. Retina 2016 Sep; 36(9): 1652–7.
13. Izumi T, Koizumi H, Maruko I, et al. Structural analyses of choroid after half-dose verteporfin photodynamic therapy for central serous chorioretinopathy. Br J Ophthalmol 2017 Apr; 101(4): 433–7.
14. Nicolò M, Rosa R, Musetti D, Musolino M, Saccheggiani M, Traverso CE. Choroidal Vascular Flow Area in Central Serous Chorioretinopathy Using Swept-Source Optical Coherence Tomography Angiography. Invest Ophthalmol Vis Sci 2017 Apr 1; 58(4): 2002–10.
15. Chan SY, Wang Q, Wei WB, Jonas JB. Optical coherence tomographic angiography in central serous chorioretinopathy. Retina 2016 Nov; 36(11): 2051–8.
16. Taban M, Boyer DS, Thomas EL, Taban M. Chronic central serous chorioretinopathy: photodynamic therapy. Am J Ophthalmol 2004 Jun; 137(6): 1073–80.
17. Silva RM, Ruiz-Moreno JM, Gomez-Ulla F, et al. Photodynamic therapy for chronic central serous chorioretinopathy: a 4-year follow-up study. Retina 2013 Feb; 33(2): 309–15.
18. Yannuzzi LA, Slakter JS, Gross NE, et al. Indocyanine green angiography-guided photodynamic therapy for treatment of chronic central serous chorioretinopathy: a pilot study. 2003. Retina 2012 Feb; 32 Suppl 1: 288–98.
19. Tsakonas GD, Kotsolis AI, Koutsandrea C, Georgalas I, Papaconstantinou D, Ladas ID. Multiple spots of photodynamic therapy for the treatment of severe chronic central serous chorioretinopathy. Clin Ophthalmol 2012; 6: 1639–44.
20. Reibaldi M, Cardascia N, Longo A, et al. Standard-fluence versus low-fluence photodynamic therapy in chronic central serous chorioretinopathy: a nonrandomized clinical trial. Am J Ophthalmol 2010 Feb; 149(2): 307–315.e2.
21. Ma DJ, Park UC, Kim ET, Yu HG. Choroidal vascularity changes in idiopathic central serous chorioretinopathy after half-fluence photodynamic therapy. PLoS One 2018 Aug 27; 13(8): e0202930.
22. Branchini LA, Adhi M, Regatieri CV, et al. Analysis of choroidal morphologic features and vasculature in healthy eyes using spectral-domain optical coherence tomography. Ophthalmology 2013 Sep; 120(9): 1901–8.
23. Iovino C, Pellegrini M, Bernabei F, et al. Choroidal Vascularity Index: An In-Depth Analysis of This Novel Optical Coherence Tomography Parameter. J Clin Med 2020 Feb 21; 9(2): 595.
24. Schlötzer-Schrehardt U, Viestenz A, Naumann GO, Laqua H, Michels S, Schmidt-Erfurth U. Dose-related structural effects of photodynamic therapy on choroidal and retinal structures of human eyes. Graefes Arch Clin Exp Ophthalmol 2002 Sep; 240(9): 748-57.
25. Husain D, Kramer M, Kenny AG, et al. Effects of photodynamic therapy using verteporfin on experimental choroidal neovascularization and normal retina and choroid up to 7 weeks after treatment. Invest Ophthalmol Vis Sci 1999 Sep; 40(10): 2322–31.
26. Schmidt-Erfurth U, Laqua H, Schlötzer-Schrehard U, Viestenz A, Naumann GO. Histopathological changes following photodynamic therapy in human eyes. Arch Ophthalmol 2002 Jun; 120(6): 835–44.
27. Maruko I, Iida T, Sugano Y, Furuta M, Sekiryu T. One-year choroidal thickness results after photodynamic therapy for central serous chorioretinopathy. Retina 2011 Oct; 31(9): 1921–7.
28. Oh BL, Yu HG. Choroidal thickness after full-fluence and half-fluence photodynamic therapy in chronic central serous chorioretinopathy. Retina 2015 Aug; 35(8): 1555–60.
29. Kim YK, Ryoo NK, Woo SJ, Park KH. Choroidal Thickness Changes After Photodynamic Therapy and Recurrence of Chronic Central Serous Chorioretinopathy. Am J Ophthalmol 2015 Jul; 160(1): 72–84.e1.
30. Demircan A, Yesilkaya C, Alkin Z. Early choriocapillaris changes after half-fluence photodynamic therapy in chronic central serous chorioretinopathy evaluated by optical coherence tomography angiography: Preliminary results. Photodiagnosis Photodyn Ther 2018 Mar; 21: 375–8.
31. Demirel S, Özcan G, Yanık Ö, Batıoğlu F, Özmert E. Vascular and structural alterations of the choroid evaluated by optical coherence tomography angiography and optical coherence tomography after half-fluence photodynamic therapy in chronic central serous chorioretinopathy. Graefes Arch Clin Exp Ophthalmol 2019 May; 257(5): 905–12.
32. Chan SY, Pan CT, Wang Q, Shi XH, Jonas JB, Wei WB. Optical coherent tomographic angiographic pattern of the deep choroidal layer and choriocapillaris after photodynamic therapy for central serous chorioretinopathy. Graefes Arch Clin Exp Ophthalmol 2019 Jul; 257(7): 1365–72.
33. Cennamo G, Montorio D, Comune C, et al. Study of vessel density by optical coherence tomography angiography in patients with central serous chorioretinopathy after low-fluence photodynamic therapy. Photodiagnosis Photodyn Ther 2020 Jun; 30: 101742.
34. Alovisi C, Piccolino FC, Nassisi M, Eandi CM. Choroidal Structure after Half-Dose Photodynamic Therapy in Chronic Central Serous Chorioretinopathy. J Clin Med 2020 Aug 24; 9(9): 2734.
35. Costanzo E, Cohen SY, Miere A, et al. Optical Coherence Tomography Angiography in Central Serous Chorioretinopathy. J Ophthalmol 2015; 2015: 134783.
36. Savastano MC, Lumbroso B, Rispoli M. In vivo characterization of retinal vascularization morphology using optical coherence tomography angiography. Retina 2015 Nov; 35(11): 2196–203.
37. Regatieri CV, Novais EA, Branchini L, et al. Choroidal thickness in older patients with central serous chorioretinopathy. Int J Retina Vitreous 2016 Sep 15; 2: 22.

38. Agrawal R, Seen S, Vaishnavi S, et al. Choroidal Vascularity Index Using Swept-Source and Spectral-Domain Optical Coherence Tomography: A Comparative Study. Ophthalmic Surg Lasers Imaging Retina 2019 Feb 1; 50(2): e26–e32.

39. Christou EE, Stavrakas P, Kozobolis V, Katsanos A, Georgalas I, Stefaniotou M. Evaluation of the choriocapillaris after photodynamic therapy for chronic central serous chorioretinopathy. A review of optical coherence tomography angiography (OCT-A) studies. Graefes Arch Clin Exp Ophthalmol 2022 Jun; 260(6): 1823–35.